ISSN : 0974 - 7486 Volume 13 Issue 6

Materials Science

An Indian Journal

Full Paper

MSAIJ, 13(6), 2015 [175-182]

# Preparation of silicate modified hydrotalcite and its influence on EVA combustion characteristics and thermal property

**Xiu-Yan Pang[1]*, Bing Liang[1,2], Yu Tian[1,3]**

**[1]College of Chemistry and Environmental Science, Hebei University, Baoding, 071002, Hebei, (PR CHINA)**

**[2]HeBei Chengxin Co.Ltd, 050083, Yuanshi County, Hebei, (PR CHINA)**

**[3]Department of Thermal Engineering, Tsinghua University, Beijing, 100084, (PR CHINA)**

**E-mail: pxy833@163.com**

## ABSTRACT

To synthesize silicate modified hydrotalcite written as Mg-Al-$SiO_3$, series synthesis methods such as co-precipitation, roasting recovery and ion exchange were tested using $Mg(NO_3)_2 \cdot 6H_2O$, $Al(NO_3)_3 \cdot 9H_2O$ and $Na_2SiO_3 \cdot 9H_2O$ as raw materials. With crystallinity and purity of product as judgment standard, co-precipitation hydrothermal method at 120°C and crystallization 24.0 h was confirmed and employed to prepare Mg-Al-$SiO_3$ flame retardant. X-ray diffraction spectroscopy (XRD), Field emission scanning electron microscope (FESEM) and Fourier transform infrared spectroscopy (FTIR) characterized its morphology, structure and functional groups. The gravimetric analysis (TG), differential thermal gravimetric (DTG) and limiting oxygen index (LOI) experiments testify that the addition of the prepared Mg-Al-$SiO_3$ hydrotalcite can decrease the thermal stability of ethylene vinyl acetate copolymer (EVA) in low temperature range, but it can obviously reduce the maximum mass loss rate and improve residual char and LOI value. It can be found by comparison experiment that Mg-Al-$CO_3$ hydrotalcite shows better flame retardancy than Mg-Al-$SiO_3$. 

## KEYWORDS

Hydrotalcite;
Silicate modified;
EVA;
Thermal stability;
Flame retardancy.

## INTRODUCTION

People have paid more attention to the use of halogen-containing flame retardants due to its production of a large amount of smoke and toxic gases during combustion. In recent years, the halogen-free flame retardants, especially the metal hydroxides[1-3], have been extensively used as low smoke and toxic-free additives. As typical metal hydroxides, magnesium hydroxide (MH) and aluminum hydroxide (ATH) are widely used as flame-retardant additives of polyolefine for manufacturing the halogen-free and low smoke insulated cables[4, 5]. These compounds act in both the condensed and gas phase through an endothermic reaction, which reduce the temperature of materials in the condensed phase and release vapour to dilute the combustible gas in the gas phase. However, they have some disadvantages such as high additive amount and poor compatibility with the polymeric matrix, which degrade the me-

chanical properties[6, 7]. Therefore, it is significant to search for some other inorganic hydroxides to replace MH and ATH.

Hydrotalcite-like compounds known as layered double hydroxides (LDHs) belong to a kind of anionic clay minerals[8]. It has the similar structure and composition to MH and ATH, so LDHs have been extensively used in the flame retardation of polymers because of their excellent advantages such as low smoke, no toxicity, no corrosive gas generation, higher flame retardancy than MH and ATH[9-11]. However, LDHs still have a fatal disadvantage of more than 60 wt% adding dosage in the composites in order to obtain an adequate level of flame retardancy properties[9, 12], which would be detrimental to the mechanical properties of flame retarded polyolefin materials because of the poor compatibility between these inorganic additives and polymer composite. In order to improve the mechanical properties, surface treatment of LDHs[13] or addition of LDHs together with other synergistic flame retardants[14-16] were test to improve flame retardancy and reduce retardant additive dosage. However, this kind of improvement of mechanical properties is not only very limited, but also the surface modification brings the deterioration of flame retardancy.

Anions in interlayer structure of LDH are exchangeable, inorganic or organic acid anions can be inserted under specific reaction condition[17] and then the modification for LDH be carried out. LDHs can be prepared with different methods such as co-precipitation[18], ion exchange[19], roasting recovery[20], template synthesis[21], in-situ synthesis[22] and microemulsion method[23]. Silicate is a kind of well-known flame retardant with good flame retardancy caused by the formation of $SiO_2$ protective layer on composite surface[24]. Meanwhile, silicate normally uses together with other flame retardants in order to improve its flame retarding property[25].

Herein, the main purpose of this research is to prepare silicate modified LDHs (written as Mg-Al-$SiO_3$) and further tests its flame retardancy. To get the optimizing synthesis method and reaction condition, X-ray diffraction spectroscopy (XRD), Field emission scanning electron microscope (FESEM) and Fourier transform infrared spectroscopy (FTIR) were used to characterize the morphology, structure and functional groups of the prepared LDHs. Thermal gravimetric (TG) and differential thermal gravimetric (DTG) analysis were employed to study the thermal stability. The flame retardancy of the synthesized LDHs for EVA was investigated by LOI tests.

## EXPERIMENTAL

### Materials and sample preparation

Natural flake graphite (average flake size of 0.18 mm, carbon content of 95%; Action Carbon CO. LTD, Baoding, China); EVA 14-2 copolymer (containing 14 wt% vinyl acetate, density of 0.935 $g \cdot cm^{-3}$ and melt flow rate 0.2 $g^{-1}$ min; Beijing East Petrochem, China). $Mg(NO_3)_2 \cdot 6H_2O$, $Al(NO_3)_2 \cdot 9H_2O$, $Na_2CO_3$, $Na_2SiO_3 \cdot 9H_2O$, $H_2SO_4$ (98%), NaOH and $KMnO_4$ were all analytical agents.

### Synthesis of Mg-Al-$CO_3$ hydrotalcite

Solution A was prepared with $Mg(NO_3)_2 \cdot 6H_2O$, $Al(NO_3)_3 \cdot 9H_2O$ and deionized water as raw materials, keeping the $Mg^{2+}/Al^{3+}$ mole ratio and the total positive ion concentration as 3:1, 1$mol \cdot L^{-1}$, respectively. The alkaline solution B of NaOH and $Na_2CO_3$ in 100 mL distilled water was prepared keeping the concentration of $[OH^-]$ as $[2.2[Mg^{2+}]+3.2[Al^{3+}]]$, and $[CO_3^{2-}]$ as $0.5[Al^{3+}]$. Ion concentration was controlled as TABLE 1. Then solution A and B were added dropwise to a beaker containing some deionized water, and the pH of the solution was controlled as 8.9~9.3 at 40°C with a vigorous stirring for about 1 hour. Then the mixture was transferred into a

**TABLE 1 : The ion concentration at different systems**

| Systems | Ion concentration (mol·L$^{-1}$) | | | | |
|---|---|---|---|---|---|
| | $Mg^{2+}$ | $Al^{3+}$ | $OH^-$ | $CO_3^{2-}$ | $SiO_3^{2-}$ |
| Mg-Al-$CO_3$ | 0.75 | 0.25 | 2.45 | 0.125 | 0 |
| Mg-Al-$SiO_3$ | 0.75 | 0.25 | 2.45 | 0 | 0.125 |

Teflon-lined hydrothermal reaction vessel and crystallized 6.0 h at 120°C. Then the precipitate was filtered, washed by deionized water and alcohol, and finally dried at 120°C, yielding white powder of Mg-Al-$CO_3$.

### Synthesis of silicate modified Mg-Al- $SiO_3$ hydrotalcite

### Co-precipitation method

Solution A was prepared as mentioned above. The alkaline solution B of NaOH and $Na_2SiO_3$ in 100 mL distilled water was prepared keeping the concentration of $[OH^-]$ as $[2.2[Mg^{2+}] + 3.2[Al^{3+}]]$, and $[SiO_3^{2-}]$ as $0.5[Al^{3+}]$. Ion concentration was controlled as TABLE 1. Then solution A and B were added dropwise to a beaker containing some deionized water, and the pH of the solution was controlled as 9.5~10. Other conditions are all the same as mention in the synthesis of Mg-Al-$CO_3$. The obtained product is written as $[Mg\text{-}Al\text{-}SiO_3]_{cop}$.

### Roasting recovery methods

The precursor Mg-Al-$CO_3$ was synthesis at first according to the method mentioned above, and then it was roasted at 500°C and turned into layered double-metal oxide (LDO). 1.0 g the obtained LDO and 2.0 g $Na_2SiO_3$ were added to 100 mL distilled water and kept at 40°C for 12.0 h, and then the solid was filtrated, dried and grinded. The obtained powder product is labeled as $[Mg\text{-}Al\text{-}SiO_3]_{roa}$.

### Ion exchange method

The precursor Mg-Al-$CO_3$ was synthesis at first and then 1.0 g Mg-Al-$CO_3$ was dissolved in $Na_2SiO_3$ water solution with a pH of 12. Keeping the reflux reaction 24.0 h at 100°C, and then the solid was filtrated, dried and grinded. The obtained powder is labeled as $[Mg\text{-}Al\text{-}SiO_3]_{exc}$.

### Measurements and characterization

### XRD analysis

XRD data were recorded with a Y-4Q X-ray diffractometer (Dandong, China) under the operation condition of 40 kV, 30 mA, employing Cu Kα radiation with a Ni filter (wavelength 0.15418 nm) with a scan rate of 0.06 °·$S^{-1}$ and 2θ ranging from 5° to 70°.

### SEM analysis

JSM-7500F field emission scanning electron microscope (Japan) was employed to observe morphology of the prepared Mg-Al- $CO_3$ and Mg-Al-$SiO_3$ hydrotalcites.

### FTIR analysis

The FTIR spectra of the prepared Mg-Al- $CO_3$ and Mg-Al- $SiO_3$ hydrotalcites were recorded between 4000-400 $cm^{-1}$ using a FTS-40FTIR spectrometer (America Biorad) with a resolution of 2 $cm^{-1}$.

### TG analysis

$N_2$ flux was controlled as 25 mL·$min^{-1}$, with about 10.0 mg sample laid in porcelain crucible, and then heated to 700°C at a rate of 10°C·$min^{-1}$. Changes of sample weight as temperature were recorded.

### LOI detection

LOI value was measured with JF-3 oxygen index instrument (Chengde, China). The incised slivers of flame retarded EVA composites with a dimension of 120×6×3 $mm^3$ were detected according to Standard of GB/T2406-1993.

## RESULTS AND DISCUSSION

### Optimization of synthesis method

In reaction, the Mg-Al subject and $SiO_3^{2-}$ object can be assembled through co-precipitation, roasting recovery and ion exchange methods. These mentioned methods are all tested and the obtained products were firstly detected with XRD instrument.

Figure 1 shows the XRD patterns of Mg-Al-$CO_3$ and Mg-Al-$SiO_3$ series synthesized with different methods. As shown in Figure 1 d, all the diffraction peaks of Mg-Al-$CO_3$ are in good agreement with layered structures and are ascribable to hydrotalcite indexed in a hexagon lattice[26]. As for Mg-Al-$SiO_3$ series, the diffraction peaks of $[Mg\text{-}Al\text{-}SiO_3]_{exc}$ shown in Figure 1 c are all the same as that of Mg-Al-$CO_3$, which testify that $SiO_3^{2-}$ ions can not efficiently insert into interlamination and replace the $CO_3^{2-}$ ions. As for $[Mg\text{-}Al\text{-}SiO_3]_{cop}$ and [Mg-Al-

Full Paper

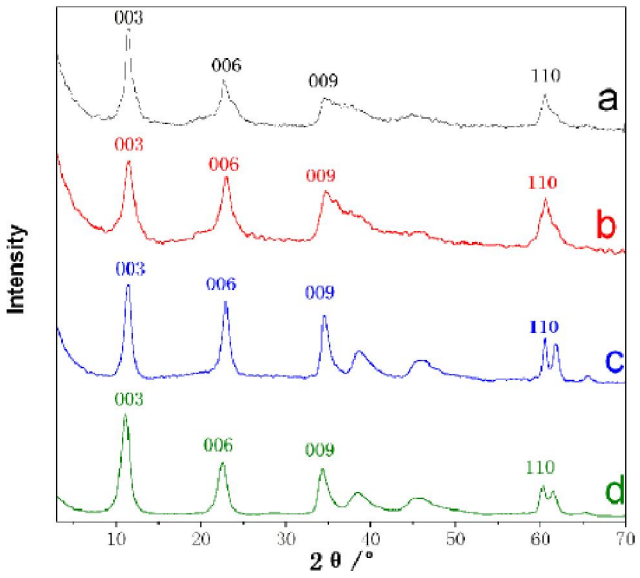


**Figure 1: XRD character of $[Mg\text{-}Al\text{-}SiO_3]_{cop}$ (a), $[Mg\text{-}Al\text{-}SiO_3]_{roa}$ (b), $[Mg\text{-}Al\text{-}SiO_3]_{exc}$ (c) and $Mg\text{-}Al\text{-}CO_3$ (d)**

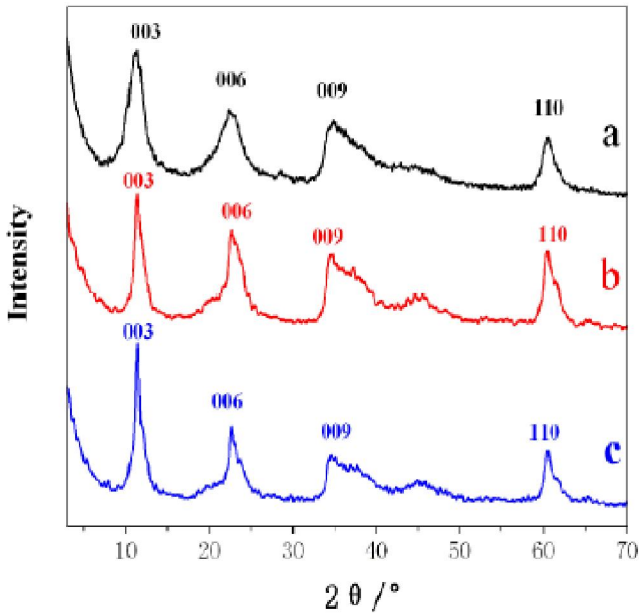


**Figure 2 : The XRD patterns of $Mg\text{-}Al\text{-}SiO_3$ hydrotalcites with different crystallization time of 6.0 h (a), 12.0 h (b) and 24.0 h (c)**

$SiO_3]_{roa}$, the pattern character is the same as $Mg\text{-}Al\text{-}SiO_3$ hydrotalcite as reported in literature[27], their crystal plane (003) correspond a crystal spacing of 7.78 nm and 7.76 nm respectively as shown in TABLE 2. According to crystal chemistry theory, the stronger of the crystal plane diffraction peak, the better formed crystal is; and the smaller of the peak full width at half height, the bigger the obtained crystal particle size is. Comparative analysis the results presented in Figure 1 a, Figure 1 b, and TABLE 2, it can be seen that the $[Mg\text{-}Al\text{-}SiO_3]_{cop}$ hydrotalcite prepared with co-precipitation method holds relatively better well-formed crystalline layered structures.

## Optimization of $Mg\text{-}Al\text{-}SiO_3$ hydrotalcite crystallization time

As testified above, $Mg\text{-}Al\text{-}SiO_3$ hydrotalcite prepared with co-precipitation method has well-formed crystalline structures; therefore, the further experiments for crystallization time were carried out with crystal purity as optimizing object. Figure 2 shows the XRD patterns of synthesized $Mg\text{-}Al\text{-}SiO_3$ specimens at 120°C corresponding different crystallization time. As can be seen, when the crystallization time is controlled as 6.0 h, the obtained solids powder already possesses the layered structures of hydrotalcite, but it holds a lower crystallinity and purity. When it is lengthened to 12.0 h or 24.0 h, crystallinity and purity of solids powders are improved, which can be testified by the smaller crystal spacing and full width at half height corresponding to the crystal plane (003) as listed in TABLE 3.

## Morphology characterization of the hydrotalcites

Morphology of $Mg\text{-}Al\text{-}CO_3$ and $Mg\text{-}Al\text{-}SiO_3$ hydrotalcites synthesized with co-precipitation method were observed, and the SEM images were shown as Figure 3. Figure 3 (a) indicated lamellar particles of $Mg\text{-}Al\text{-}CO_3$ hydrotalcite looked like rounded hexagonal shapes, which is typical of hydrotalcite-like materials[30] and with a lateral size of the platelet less than 200 nm. Compared with $Mg\text{-}Al\text{-}CO_3$, although $Mg\text{-}Al\text{-}SiO_3$ hydrotalcite particles

**TABLE 2 : XRD patterns data of $Mg\text{-}Al\text{-}SiO_3$ hydrotalcites**

| Specimens | $d_{(003)}$/nm | $W_{1/2}$/rad |
|---|---|---|
| $[Mg\text{-}Al\text{-}SiO_3]_{cop}$ | 7.78 | 1.047 |
| $[Mg\text{-}Al\text{-}SiO_3]_{roa}$ | 7.76 | 1.290 |
| $[Mg\text{-}Al\text{-}SiO_3]_{exc}$ | 7.84 | 0.925 |

**TABLE 3 : XRD patterns data of Mg-Al-$SiO_3$ hydrotalcites with different crystallization time**

| Specimens | $d_{(003)}$/nm | $W_{1/2}$/rad |
|---|---|---|
| $[Mg\text{-}Al\text{-}SiO_3]_{6h}$ | 7.97 | 2.187 |
| $[Mg\text{-}Al\text{-}SiO_3]_{12h}$ | 7.84 | 1.113 |
| $[Mg\text{-}Al\text{-}SiO_3]_{24h}$ | 7.80 | 1.087 |

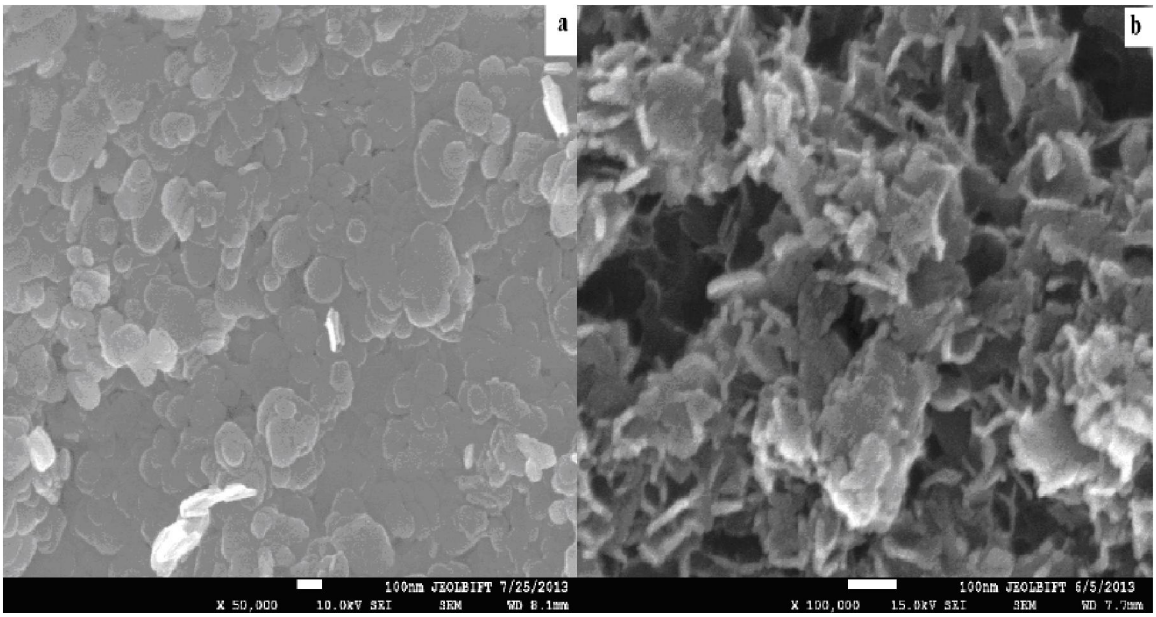


**Figure 3 : SEM morphology of Mg-Al-$CO_3$ (a) and Mg-Al-$SiO_3$ (b) hydrotalcites**

present rounded hexagonal shapes, they emerge a bad shape definition, surface regularity and size uniformity, and there is serious agglomeration of particles at the same time.

## FTIR characterization of Mg-Al-$CO_3$ and Mg-Al-$SiO_3$ hydrotalcites

The FTIR spectra of Mg-Al–$CO_3$ and Mg-Al–$SiO_3$ hydrotalcites are shown in Figure 4. The broad band around 3500 $cm^{-1}$, observed in Mg-Al–$CO_3$ (A) and Mg-Al–$SiO_3$ (B) simultaneously, is the stretching mode of hydroxyl groups attached to metal ions of Mg and Al in the layers, and the bands close to 1630 $cm^{-1}$ are assigned to the bending vibration of interlayer water molecules. The narrower absorption peak at 1360-1390$cm^{-1}$ in Figure 4 (A) and (B) is attributed to the asymmetric $v_3$ vibration of interlayer $CO_3^{2-}$, which testifies some $CO_3^{2-}$ ions contained in Mg-Al–$SiO_3$ hydrotalcite caused by the $CO_2$ in air. However, there is a wide and strong absorption peak at 1010 $cm^{-1}$ in FTIR spectra of Mg-Al–$SiO_3$, which corresponds to anti-symmetric and symmetric stretching vibrations bands of Si-O-Si[31]. Bands at lower wave numbers (600–690 $cm^{-1}$) might be attributed to the overlap of the asymmetric $v_4$ vibration modes of $CO_3^{2-}$ and the stretching vibrations including M–O, M–O–M, and O–M–O bands in the layer.

## Thermal stability of hydrotalcites and flame retarded EVA composites

The thermal stability of a flame retarded polymeric material is extremely important, which is mainly concerned about the release of decomposition products and the formation of char. Figure 5 indicates the TG curve of Mg-Al-$CO_3$ and Mg-Al-$SiO_3$ hydrotalcites, EVA and flame retarded EVA; some thermoanalysis data are listed in TABLE 4 at the same time. It can be seen from the given results that although the addition of Mg-Al-$CO_3$ or Mg-Al-$SiO_3$ decrease the thermal stability of EVA in low temperature range indicated by initial decomposition temperature $T_1$ and $T_5$, it can reduce the maximum mass loss rate ($R_{max}$) simultaneously. It's worthy noting that the addition of these flame retardants can obviously improve the residual char caused by

Full Paper

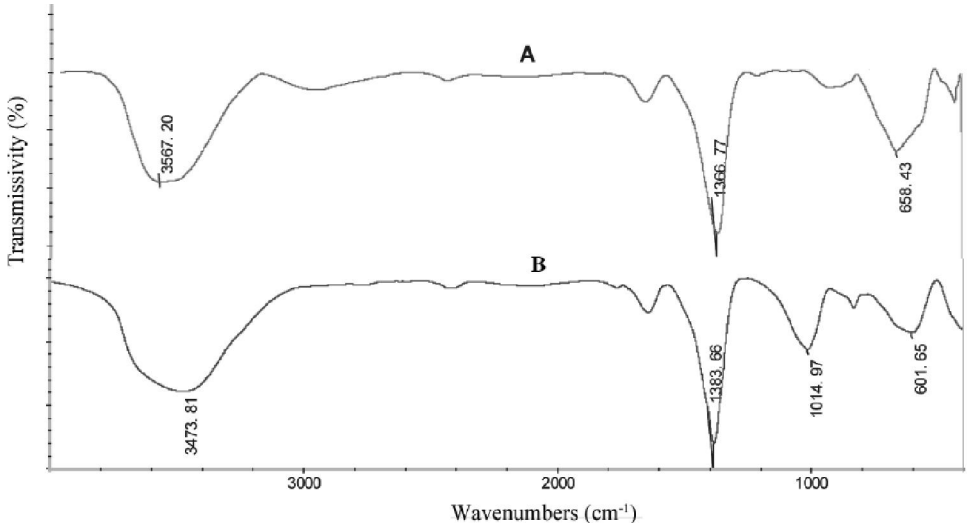


**Figure 4 : FTIR character of Mg-Al-$CO_3$ (A) and Mg-Al-$SiO_3$ (B) hydrotalcites**

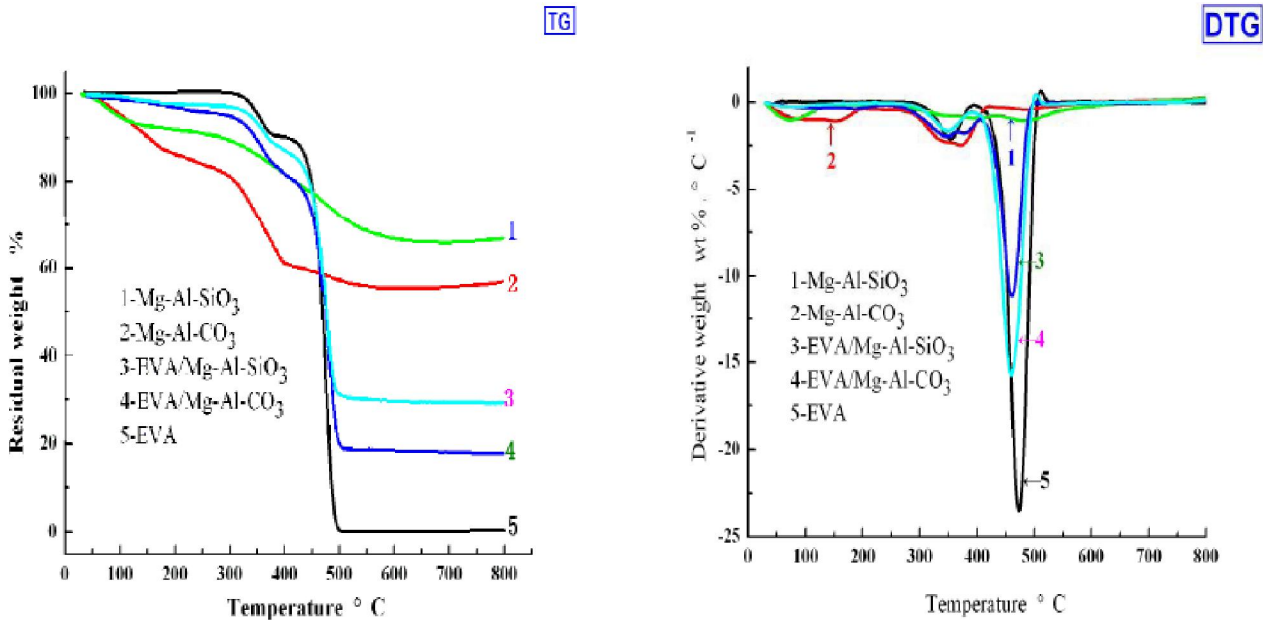


**Figure 5 : The TG and DTG curves of hydrotalcites and flame retarded EVA composites**

the decomposition product of Mg-Al-$CO_3$ or Mg-Al-$SiO_3$ hydrotalcite. Furthermore, Mg-Al-$SiO_3$ holds a lower $R_{max}$ and a higher residual char yield than Mg-Al-$CO_3$.

## Effect of flame retardants on the LOI value of EVA blends

TABLE 5 lists the LOI values of EVA composites with and without synergists. It can be seen that the LOI values of pure EVA is only 19.3%. LOI values of EVA with synergists are all higher than that of pure EVA. Addition of $Mg(OH)_2$ and $Al(OH)_3$ (at a mass ratio of 22.5:7.5) with a total mass fraction of 30% lead LOI value of EVA blends to 24.2%. However, the addition of the same amount of the prepared Mg-Al-$SiO_3$ into EVA improves the LOI to 25.8%. The good flame retardancy of Mg-Al-$SiO_3$ should be attributed to the formation of solid decomposition products of $SiO_2$, MgO and $Al_2O_3$, which cover on the base material surface and inhibits the transfer of heat and mass. Although the Mg-Al-$CO_3$ retarded EVA holds lower residual char yield than EVA/Mg-Al-$SiO_3$ system, it presents a little better flame retardancy. The results may be caused by its simultaneous gas phase and condensed phase flame-retardation effect. Mg-Al-$CO_3$ will consume heat energy and release $H_2O$ and $CO_2$, which

**TABLE 4 : Thermoanalysis data of specimens in $N_2$ atmosphere**

| Specimens | $T_1$ ℃ | $T_5$ ℃ | $R_{max}$ wt%·min$^{-1}$ | Residual char yield % |
|---|---|---|---|---|
| Mg-Al-$SiO_3$ | 52 | 97 | -1.093 | 66.84 |
| Mg-Al-$CO_3$ | 58 | 105 | -2.470 | 56.93 |
| EVA/Mg-Al-$SiO_3$ | 119 | 339 | -12.08 | 29.40 |
| EVA/Mg-Al-$CO_3$ | 81 | 299 | -18.44 | 17.84 |
| EVA | 328 | 352 | -25.76 | 0.34 |

**$T_1$: the initial decomposition temperature (IDT) corresponding to a 1% weight loss, °C; $T_5$: the initial decomposition temperature (IDT) corresponding to a 5% weight loss, °C; $R_{max}$: the maximum mass loss rate, wt%·min$^{-1}$**

**TABLE 5 : LOI of the flame retarded EVA blends**

| Components mass percentage % | | | | | LOI/% |
|---|---|---|---|---|---|
| EVA | Mg-Al-$CO_3$ | Mg-Al-$SiO_3$ | $Mg(OH)_2$ | $Al(OH)_3$ | |
| 100 | 0 | 0 | 0 | 0 | 19.3 |
| 70 | 30 | 0 | 0 | 0 | 27.0 |
| 70 | 0 | 30 | 0 | 0 | 25.8 |
| 70 | 0 | 0 | 0 | 0 | 26.5 |
| 70 | 0 | 0 | 22.5 | 7.5 | 24.2 |

decreases the temperature of the flame zone and dilutes the flammable gases and oxygen. At the same time, the formed metal oxide residues of MgO and $Al_2O_3$ can block the burning process by reducing the oxygen and heat supplied to the bulk phase. It can be seen $CO_3^{2-}$ in hydrotalcite plays more important role in flame retardancy of EVA.

## CONCLUSIONS

Silicate modified hydrotalcite can be prepared with co-precipitation hydrothermal method at 120°C and crystallization 24.0 h. XRD, SEM and FTIR have characterized its lamellar structure, rounded hexagonal shapes and functional group. The prepared Mg-Al-$SiO_3$ hydrotalcite can obviously reduce the maximum mass loss rate of EVA composite and improve its residual char and LOI value. The good flame retardancy should be attributed to the formation of $SiO_2$, MgO and $Al_2O_3$ in condensed phase. Mg-Al-$CO_3$ hydrotalcite presents a little better flame retardancy than Mg-Al-$SiO_3$.

## ACKNOWLEDGEMENTS

This study is supported by Seedling Project of College of Chemistry and Environmental Science. At the same time, we gratefully acknowledge the support of Undergraduate Laboratory Project of Hebei University.

## REFERENCES

**[1]** Y.Y.Yen, H.T.Wang, W.J.Guo; Polym.Degrad.Stab., **97**, 863 **(2012)**.
**[2]** Z.Z.Li, B.J.Qu; Polym.Degrad.Stab., **81**, 401 **(2003)**.
**[3]** L.Haurie, A.I.Fernández, J.I.Velasco, J.M.Chimenos, J.M.L.Cuesta; F.Espiell, Polym.Degrad. Stabil., **92**, 1082 **(2007)**.
**[4]** J.Lv, L.Qiu, B.Qu; Nanotechnology, **15**, 1576 **(2004)**.
**[5]** B.M.Alexander, W.G.Jeffrey; Fire Mater., **37**, 259 **(2013)**.
**[6]** Z.Wang, B.Qu, W.Fan, P.Huang; J.Appl.Polym.Sci., **81**, 206 **(2001)**.
**[7]** R.N.Rothon, P.R.Hornsby; Polym.Degrad.Stab., **54**, 383 **(1996)**.
**[8]** L.M.Parker, N.B.Milestone, R.H.Newman; Ind.Eng.Chem.Res., **34**, 1196 **(1995)**.
**[9]** C.M.Jiao, Z.Z.Wang, Z.Ye, Y.Hu, W.C.Fan; J.Fire.Sci., **24**, 47 **(2006)**.
**[10]** F.Cavani, F.Trifirò, A.Vaccari; Catalysis today, **11**, 173 **(1991)**.

Full Paper

**[11]** C.M.Jiao, X.L.Chen; J.Appl.Polym.Sci., **120**, 1285 **(2011)**.
**[12]** L.C.Du, Y.C.Zhang, X.Y.Yuan, J.Y.Chen; Polym.Plastics Technol.Eng., **48**, 1002 **(2009)**.
**[13]** C.X.Jia, Y.Qian, X.L.Chen, Y.Liu; Polym.Eng.Sci., **12**, 2918 **(2014)**.
**[14]** L.Ye, P.Ding, M.Zhang, B.J.Qu; J.Appl.Polym.Sci., **107**, 3694 **(2008)**.
**[15]** L.Li, Y.Qian, C.M.Jiao; Polym.Eng.Sci., **54**, 766 **(2014)**.
**[16]** Z.Z.Wang, B.J.Qu, W.C.Fan, Z.Li; J.Funct.Polym., **14**, 45 **(2001)**.
**[17]** C.M.Jiao, Z.Z.Wang, X.L.Chen, Y.H; J.Appl.Polym.Sci., **107**, 2626 **(2008)**
**[18]** J.M.Oh, S.H.Hwang, J.H.Choy; Solid State Ionics, **151**, 285 **(2002)**.
**[19]** Z.P.Xu, P.S.Braterman; J.Mater.Chem., **13**, 268 **(2003)**.
**[20]** S.Carlino, J.M.Hudson, S.W.Husain, J.A.Knowles; Solid State Ionics, **84**, 117 **(1996)**.
**[21]** J.He, B.Li, D.G.Evans, X.Duan; Colloid.Surface.A, **251**, 191 **(2004)**.
**[22]** S.B.Mao, D.Q.Li, F.Z.Zhang, G.E.David, X.Duan; Chinese Inorg.Chem.Acta, **20**, 596 **(2004)**.
**[23]** A.I.Khan, D.O.Hare; J.Mater.Chem., **12**, 3191 **(2002)**.
**[24]** Z.Hu, L.Chen, B.Zhao, Y.Luo, D.Y.Wang, Y.Z.Wang; Polym.Degrad.Stabil., **96**, 320 **(2011)**.
**[25]** B.Schartel, A.Wei, F.Mohr, M.Kleemeier, A.Hartwig, U.Braun; J.Appl.Polym.Sci., **118**, 1134 **(2010)**.
**[26]** H.Pfeiffer, E.Lima, V.Lara, J.S.Valente; Langmuir, **26**, 4074 **(2010)**.
**[27]** C.Misra, A.JPerrotta; Clay.Clay Miner., **40**, 145 **(1992)**.